

## Refining glass structure in two dimensions

Mahdi Sadjadi\*

*Department of Physics, Arizona State University, Tempe, Arizona 85287-1604, USA*

Bishal Bhattarai† and D. A. Drabold‡

*Department of Physics and Astronomy, Ohio University, Athens, Ohio 45701, USA*

M. F. Thorpe§

*Department of Physics, Arizona State University, Tempe, Arizona 85287-1604, USA  
and Rudolf Peierls Centre for Theoretical Physics, University of Oxford, 1 Keble Road, Oxford OX1 3NP, United Kingdom*

Mark Wilson||

*Department of Chemistry, Physical and Theoretical Chemistry Laboratory, University Of Oxford, South Parks Road,  
Oxford OX1 3QZ, United Kingdom*

(Received 7 July 2017; revised manuscript received 8 September 2017; published 10 November 2017)

Recently determined atomistic scale structures of near-two dimensional bilayers of vitreous silica (using scanning probe and electron microscopy) allow us to refine the experimentally determined coordinates to incorporate the known local chemistry more precisely. Further refinement is achieved by using classical potentials of varying complexity: one using harmonic potentials and the second employing an electrostatic description incorporating polarization effects. These are benchmarked against density functional calculations. Our main findings are that (a) there is a symmetry plane between the two disordered layers, a nice example of an emergent phenomena, (b) the layers are slightly tilted so that the Si-O-Si angle between the two layers is not  $180^\circ$  as originally thought but rather  $175 \pm 2^\circ$ , and (c) while interior areas that are not completely imagined can be reliably reconstructed, surface areas are more problematic. It is shown that small crystallites that appear are just as expected statistically in a continuous random network. This provides a good example of the value that can be added to disordered structures imaged at the atomic level by implementing computer refinement.

DOI: [10.1103/PhysRevB.96.201405](https://doi.org/10.1103/PhysRevB.96.201405)

The atomic structure of covalent network glasses has been a subject of both experimental and theoretical interest since the introduction of the continuous random network (CRN) model by Zachariasen [1]. Almost all of these studies have focused on the pair distribution function (PDF) which is the Fourier transform of a diffraction pattern [2]. Experimental diffraction studies offer useful information, in particular regarding pairwise ordering [3]. However, simulation models can greatly aid the interpretation of these data as the atom positions are known unequivocally. As a result, information such as the ring statistics, which is in many ways a natural language for discussing network structure [4–6], is directly accessible. While this work has been very informative and clearly established the correctness of the CRN model for materials like vitreous silica, it is not accurate enough to distinguish between different models with varying ring statistics, etc. This situation has changed recently with the direct imaging of bilayers of silica [7,8] that has provided detailed information regarding atomic positions.

Silica,  $\text{SiO}_2$ , represents an archetypal network-forming material. At ambient pressure the crystalline and amorphous structures can be considered as constructed from

corner-sharing  $\text{SiO}_4$  tetrahedral coordination polyhedra (CP) which link to form a network. The complex linking of the CP may result in significant ordering on length scales beyond the short-range ordering imposed by the system electrostatics (effectively controlled by the relative atom electronegativities) [9–14].

Recently developed synthetic pathways have allowed thin films of  $\text{SiO}_2$  to be deposited on either metallic [7,15,16] or graphitic [8] substrates while advances in imaging techniques allow for true atomic resolution of the surface structure. Albeit, because the bilayer is a glassy material, it is not commensurate with any substrate, and so we do not include the substrate explicitly here.

Some of the thinnest films deposited are bilayers of corner-sharing  $\text{SiO}_4$  CP in which all of the Si and O atoms obtain their full (four- and two-, respectively) coordination numbers. Amorphous and crystalline films have been grown with both states characterized by the presence of a mirror plane (which houses a layer of O atoms which act as bridges between the two monolayers [17]). Critically, the pseudo-two-dimensional nature of these systems allows the ring structures to be directly observed and hence offers a potentially unique insight into the origin of any ordering on long length scales. Silica can be considered as a network of silicon atoms in which the nearest-neighbor Si-Si pairs are *dressed* with O atoms. As a result, the crystalline system can be considered as constructed exclusively from a net of six-membered (Si-Si-Si...) rings, while the amorphous systems are constructed from a distribution of 4- to 10-membered rings

\*mahdisadjadi@asu.edu

†bb248213@ohio.edu

‡drabold@ohio.edu

§mft@asu.edu

||mark.wilson@chem.ox.ac.uk

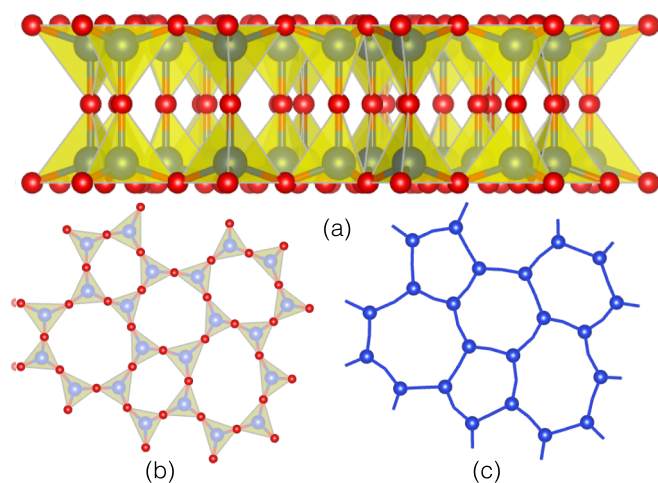


FIG. 1. (a) Small piece of silica bilayer in which oxygen atoms (red) form a tetrahedral network while silicons (blue) are located at the center of tetrahedra. (b) The top view of the silica bilayer where O and Si atoms are projected into the plane, with O forming a network of corner-sharing triangles. (c) An alternative view where Si atoms form a network of edge-sharing polygons (rings), while oxygens are removed for clarity. This view is stressed in Fig. 2.

(Fig. 1). However, this experimental information, while ground breaking, is naturally imperfect as the location of each atom has associated with it a natural uncertainty which translates into an uncertainty in atom-atom separations.

In this Rapid Communication, we show how value can be added by combining the experimental image with computer refinement that builds in the known local chemistry. While no refinement of the experimental data is required in order to obtain, for example, accurate ring statistics, refinement is required in order to address the geometrical issues associated with the network. For example, value can be added on the effect of the presence of significant unimaged regions as well as on the subtle variations in the structure perpendicular to the resolved plane containing the bilayer.

In this Rapid Communication we focus on a single large sample of a bilayer of vitreous silica imaged by the Cornell group [8] which we will refer to as sample *h*, shown in Fig. 2, to distinguish it from previous smaller experimental and computer-generated samples [18]. The sample is  $\sim 270 \times 270 \text{ \AA}^2$  in an area containing 19330 O and 9492 Si atoms, and is the largest such sample imaged at the atomic level of which we are aware.

Importantly, we are using the whole experimental sample, including voids, rather than selecting a more rectangular shaped section without voids, which would have thrown out most of the experimental data. This is also significant as the full configuration shows a number of interesting features. For example, there are several regions which may be considered nanocrystalline showing relatively large numbers of neighboring six-membered rings (highlighted by green circles with a diameter of  $9 \text{ \AA}$ ). Such regions are to be expected statistically in a CRN and from previous studies [6] we find that about 50% of all rings are sixfold and of these about 2% are surrounded by 6 sixfold rings leading to a little *microcrystallite* of 7 sixfold rings. The total number of rings in the Cornell

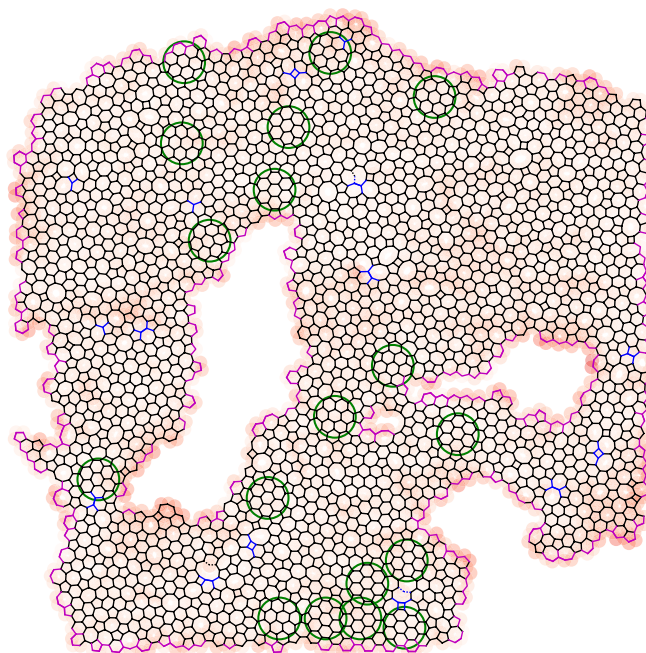


FIG. 2. Cornell *h* network viewed perpendicular to the plane containing the bilayer with the O atoms removed for clarity, and only the top layer of Si atoms shown as *vertices*. The atoms associated with the blue and magenta bonds were not directly imaged but have been added in the computer refinement. The blue and magenta bonds highlight bonds reconstructed within the main body of the sample and at the surface, respectively. Dashed lines highlight small sections in which an undercoordinated Si atom was required for filling. The intensity of the red highlights the difference between the configuration relaxed with the spring and PIM potentials. The green circles show small *crystallites*.

*h* sample is 1811, where we exclude surface rings that do not have their full compliment of neighboring rings. Thus we expect  $1811 \times 0.5 \times 0.02 \approx 18$  of such regions which is fortuitously exactly the number of regions shown by green circles. So this certainly cannot be taken as any evidence for microcrystallites as has been postulated at various times since the original ideas of Lebedev and co-workers [19].

More obviously the configuration shows three relatively large regions which were unable to be imaged (of approximate dimensions  $160 \times 40 \text{ \AA}^2$ ,  $50 \times 20 \text{ \AA}^2$ , and  $10 \times 10 \text{ \AA}^2$ , respectively) which resist reasonable attempts at computational filling (see below). A potential implication is that the underlying surface (on which the bilayer has been grown) in some way distorts the bilayer thus preventing effective imaging or perhaps the network was never formed in these regions because of surface roughness.

To construct the bilayer from the experimental image, O atoms (which are not imaged) are placed midway between Si atoms (which are imaged) thus forming a network of corner-sharing  $\text{O}_3$  triangles (each of which has an Si atom at the center). The Si and O atom planes are then separated, forming trigonal pyramids with Si atoms at the apices. A mirror image of these pyramids is joined to the original via O-atom bridges to form the completed bilayer, resulting in an initial set of  $180^\circ$  Si-O-Si bond angles centered around the

O atoms in the mirror plane (Fig. 1). An important question involves the experimental length metric to ensure the correct calibration of the image. We calculated the mean average length of the imaged nearest neighbor Si-Si distances as 3.097 Å, which is close to the expected value of 3.100 Å for glassy silica structures [20], confirming the overall accuracy of the experiment, and alleviating the need for any length rescaling. To reconstruct the unimaged regions, we use mean bond length and internal angles of rings to find the correct local topology. The subsequent relaxation of the bilayer will fix the geometry ensuring the proper bond length and angles.

This relaxation is carried out using model potentials of increasing complexity. In the simplest case, the nearest-neighbor O-O bonds are mimicked by harmonic springs with lengths set as the mean average (2.645 Å). This ensures that the system does not have any internal degrees of freedom and is minimally rigid or isostatic [21,22]. A hardcore potential is added to prevent overlap of O atoms from different tetrahedra as well as a root-mean-square deviation (RMSD) term which penalizes deviation from the experimental coordinates. This RMSD term is the sum of squares of the refined coordinates minus the experimental atomic positions and is important as this maintains the overall area and alleviates the need for additional boundary conditions to maintain the sample area. Although proper boundary conditions for finite pieces of amorphous systems can be designed [23], this simple potential can account for structural information extracted in this Rapid Communication. Maintaining the configurational area is critical in avoiding, for example, unphysical overlaps in nearest-neighbor tetrahedra in the absence of formal (electrostatic) repulsions. The balance of the surface extension and the intertetrahedral repulsions define an effective flexibility window of acceptable structural solutions, of the type commonly associated with zeolites [24]. As a result, samples with irregular boundary conditions are not a problem.

The second classical model applied is a polarizable-ion model (PIM) [25], specifically the TS potential [26] which utilizes pair potentials to model the Coulomb, short-range (overlap) and dispersive interactions. The potential employs a combination of reduced ion charges and anion dipole polarization (as described in Ref. [25]). The results from the harmonic potential model are used as the input with the PIM further refining the results.

The most sophisticated method applied uses density functional theory (DFT). However, the method is too computationally demanding to apply to the experimental Cornell *h* configuration. Therefore, a relatively small 1200 atom periodic computer-generated model (with 200 Si atoms in each monolayer) of a vitreous silica bilayer [27] was used. Density functional calculations were undertaken with the code SIESTA [28], with single-zeta basis and the local density approximation. Relaxation with a variable cell area resulted in very little change. Stability of the relaxed model was also verified [29].

The result of the PIM refinement of Cornell *h* is shown in Fig. 2. The blue (bulk) and magenta (surface) bonds have been computer reconstructed, as described earlier. The interior reconstruction was deemed to be successful, as the differences between the spring and PIM models were minor. These differences are shown by the red shading where the darkest

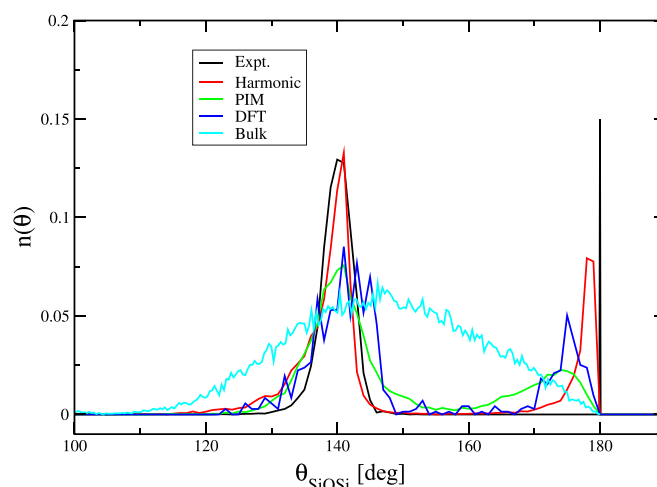


FIG. 3. Si-O-Si bond angle distributions determined from the original experimental configuration and from the bilayers obtained using models of increasing complexity as well as for the bulk glass. The peak at  $\theta_{\text{SiO}_2\text{Si}} \sim 145^\circ$  arises from the “in-plane” tetrahedral links while the peak at  $\sim 180^\circ$  arises from the central bridging oxygen atoms between the two planes. The unrefined experimental result for the Cornell *h* sample is shown in black where it was assumed that the central bridging angle was exactly  $180^\circ$ . The DFT calculation is on a computer-generated periodic sample and acts as the best guide for what to expect. The other two results are for the refined Cornell *h* sample using both the harmonic model and the polarizable-ion model as described in the text. Both show significant tilting as expected from the results of DFT, while maintaining the central symmetry plane.

red corresponds to an atomic displacement of  $\sim 0.5$  Å from the original (unrefined) coordinates. This strongly suggests that the network existed in these interior areas but was not imaged reliably, rather than the networks growing around a pillar or avoiding surface roughness on the substrate and never existing. At the surface, the difference between the spring and PIM models was much greater as the reconstruction was not contained within a small closed exterior perimeter.

In addition to in-plane information, refinement can provide valuable information in the perpendicular direction. As a benchmark of our model potentials, we have studied the Si-O-Si angle,  $\theta_{\text{SiO}_2\text{Si}}$ , as this contains important information on how the tetrahedra are linked. Figure 3 shows the distributions of  $\theta_{\text{SiO}_2\text{Si}}$  for three models. The experimental structure (in which linear Si-O-Si bridges between the two monolayers are imposed) shows a bond angle of  $\theta_{\text{SiO}_2\text{Si}} \sim 140.3^\circ$  (with a FWHM of  $\Delta\theta \sim 5.2^\circ$ ) in the bilayer plane. All of the models generate bimodal distributions in which the peak at  $\theta_{\text{SiO}_2\text{Si}} \sim 145^\circ$  may be assigned to the Si-O-Si triplets in the bilayer plane while the peaks at  $\theta_{\text{SiO}_2\text{Si}} > 175^\circ$  correspond to the triplets centered around the bridging O atoms in the mirror plane (i.e., perpendicular to the bilayer plane). There is not much latitude in the in-plane values of this angle as they must be consistent with the measured area and the known Si-O bond lengths, which leads to a single peak in the  $\theta_{\text{SiO}_2\text{Si}} \sim 145^\circ$ . Figure 3 shows that the harmonic model reproduces the important high-angle peak at  $\theta \sim 178.5^\circ$ . The lower-angle peak is at  $\theta \sim 140.9^\circ$  ( $\Delta\theta \sim 3.8^\circ$ ) and some way below the DFT result.

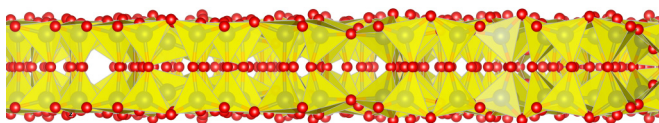


FIG. 4. Section of the Cornell  $h$  network shown along the plane containing the bilayer with O atoms shown in red, and with Si atoms at the center of the yellow tetrahedra. Note the symmetry plane of the central O atoms and also the tilting of the tetrahedra away from the vertical about the central plane.

The figure also shows the analogous distribution obtained from the bulk glass at ambient pressure using PIM, which is similar to distributions observed in bulk silicates [30,31]. The bulk distribution is significantly broader than those generated for the bilayer with  $\theta \sim 145^\circ$  and  $\Delta\theta \sim 36^\circ$ . The requirement for the relatively obtuse bond angles which characterize the links between the two layers constrains the in-plane bond angles to a relatively narrow range. For the intralayer angles all of the models show peaks at  $\theta \sim 140\text{--}142^\circ$  with the harmonic potential showing a far sharper retaining the symmetry plane.

However, the bridging O angle is tilted and reduced to about  $175.1^\circ$ . A Si-O-Si angle of  $180^\circ$  sits on a local energy maximum [32] and, as a result, tilting is inevitable. A tilt in the interlayer bond angle is observed in all the models. At the simplest level (harmonic potential) a relatively small deviation from linear ( $\theta \sim 178.5^\circ$ ) is shown. As greater detail is added to the models these angles become more acute with both the PIM and DFT results showing peaks at  $\theta \sim 175^\circ$ . Figure 4 shows the configuration perpendicular to the plane containing the bilayer relaxed using the PIM and clearly showing the tilted corner-sharing tetrahedra, with a peak at  $\theta \sim 174.9^\circ$ .

At first sight this suggests an incompatibility with the experimental results where only a single layer is seen, with the second layer of Si tetrahedra being exactly behind and underneath the first. However, this can be maintained if there is a symmetry plane involving the central O atoms, such that the upper and lower tetrahedra tilt and pucker in the same way and there is not a second image when the bilayer is imaged from above, as shown in Fig. 4. This conclusion is supported by an entropy argument in which the bilayer *with* a mirror plane is able to explore configurational space more effectively than one without [17]. There are more degrees of freedom with the symmetry plane present, thus increasing the entropy and lowering the free energy, and hence leading to this

unexpected emergent phenomena. Thus symmetry is induced in a system which at first sight seems a canonical example of a system without symmetry. This argument is confirmed both by detailed atomic computer modeling and by experiment, where no *shadow* is seen beside each atom imaged, so that the second layer must be exactly behind the first layer.

A feature to notice from Fig. 2 is that the polygons with silicon atoms at the corners appear regular, having areas close to that of regular polygons as has been previously noted [18]. This feature has been absent in computer generated models of vitreous silica bilayer as the Si-O-Si angle of around  $145^\circ$  in the plane is hard to achieve in models while maintaining the maximal convexity of Si polygons. Nature has found a way and we need to understand better how this is achieved. Note there is no difficulty in achieving regular polygons in samples of amorphous As [27] where there are no bridging atoms with which to contend.

In this Rapid Communication we have described how computer-refinement can add value to experimental images of disordered structures at the atomic level. Although here this has been attempted with an amorphous structure, with advances in imaging, many more such systems are expected to be imaged in the near future. This somewhat parallels the procedures employed to rationalize protein structure where the local chemistry, via bond lengths, etc., is included to produce the best possible structure [33]. We have shown that simple potentials are adequate here, and as well as producing refined coordinates for the bilayer (available upon request), we have shown that the two layers are tilted while maintaining a flat central symmetry plane of O atoms between the upper and lower parts of the bilayer. It is remarkable that such symmetry can exist in disordered system and this can be viewed as a clean example of an emergent phenomena.

Future work will help determine how ubiquitous bilayer structures of this type may be. It is possible, for example, that forming such structures for systems such as  $\text{GeO}_2$  may be more problematic as a significantly larger tilt ( $\theta \ll 180^\circ$ ) would have to be accommodated [32].

We would like to thank Berlin and Cornell groups for the coordinates of their networks and for useful discussions. This work used the Extreme Science and Engineering Discovery Environment (XSEDE), which is supported by National Science Foundation Grant No. ACI-1548562 [34]. Support through NSF Grants No. DMS 1564468(M.F.T.) and No. DMR 1506836(D.A.D.) is gratefully acknowledged.

- [1] W. H. Zachariasen, The atomic arrangement in glass, *J. Am. Chem. Soc.* **54**, 3841 (1932).
- [2] A. C. Wright and M. F. Thorpe, Eighty years of random networks, *Phys. Status Solidi B* **250**, 931 (2013).
- [3] H. E. Fischer, A. C. Barnes, and P. S. Salmon, Neutron and x-ray diffraction studies of liquids and glasses, *Rep. Prog. Phys.* **69**, 233 (2005).
- [4] C. S. Marians and L. W. Hobbs, Local structure of silica glasses, *J. Non-Cryst. Solids* **119**, 269 (1990).
- [5] A. Zeidler, K. Wezka, R. F. Rowlands, D. A. J. Whittaker, P. S. Salmon, A. Polidori, J. W. E. Drewitt, S. Klotz, H. E. Fischer,

- M. C. Wilding *et al.*, High-Pressure Transformation of  $\text{SiO}_2$  Glass from a Tetrahedral to an Octahedral Network: A Joint Approach using Neutron Diffraction and Molecular Dynamics, *Phys. Rev. Lett.* **113**, 135501 (2014).
- [6] M. Sadjadi and M. F. Thorpe, Ring correlations in random networks, *Phys. Rev. E* **94**, 062304 (2016).
- [7] L. Lichtenstein, C. Buechner, B. Yang, S. Shaikhutdinov, M. Heyde, M. Sierka, R. Włodarczyk, J. Sauer, and H.-J. Freund, The atomic structure of a metal-supported vitreous thin silica film, *Angew. Chem., Int. Ed. Engl.* **51**, 404 (2012).

- [8] P. Y. Huang, S. Kurasch, A. Srivastava, V. Skakalova, J. Kotakoski, A. V. Krashennikov, R. Hovden, Q. Mao, J. C. Meyer, J. Smet, D. A. Muller, and U. Kaiser, Direct imaging of a two-dimensional silica glass on graphene, *Nano Lett.* **12**, 1081 (2012).
- [9] P. S. Salmon, R. A. Martin, P. E. Mason, and G. J. Cuello, Topological versus chemical ordering in network glasses at intermediate and extended length scales, *Nature (London)* **435**, 75 (2005).
- [10] P. S. Salmon, Moments of the Bhatia–Thornton partial pair-distribution functions, *J. Phys.: Condens. Matter* **17**, S3537 (2005).
- [11] P. S. Salmon, The structure of tetrahedral network glass forming systems at intermediate and extended length scales, *J. Phys.: Condens. Matter* **19**, 455208 (2007).
- [12] P. S. Salmon, A. C. Barnes, R. A. Martin, and G. J. Cuello, Glass Fragility and Atomic Ordering on the Intermediate and Extended Range, *Phys. Rev. Lett.* **96**, 235502 (2006).
- [13] P. S. Salmon, A. C. Barnes, R. A. Martin, and G. J. Cuello, Structure of glassy GeO<sub>2</sub>, *J. Phys.: Condens. Matter* **19**, 415110 (2007).
- [14] M. Wilson, Structure and dynamics in network-forming materials, *J. Phys.: Condens. Matter* **28**, 503001 (2016).
- [15] J. Weissenrieder, S. Kaya, J.-L. Lu, H.-J. Gao, S. Shaikhutdinov, H.-J. Freund, M. Sierka, T. K. Todorova, and J. Sauer, Atomic Structure of a Thin Silica Film on a Mo (112) Substrate: A Two-Dimensional Network of SiO<sub>4</sub> Tetrahedra, *Phys. Rev. Lett.* **95**, 076103 (2005).
- [16] D. Löffler, J. J. Uhlrich, M. Baron, B. Yang, X. Yu, L. Lichtenstein, L. Heinke, C. Büchner, M. Heyde, S. Shaikhutdinov *et al.*, Growth and Structure of Crystalline Silica Sheet on Ru (0001), *Phys. Rev. Lett.* **105**, 146104 (2010).
- [17] M. Wilson, A. Kumar, D. Sherrington, and M. F. Thorpe, Modeling vitreous silica bilayers, *Phys. Rev. B* **87**, 214108 (2013).
- [18] A. Kumar, D. Sherrington, M. Wilson, and M. F. Thorpe, Ring statistics of silica bilayers, *J. Phys.: Condens. Matter* **26**, 395401 (2014).
- [19] A. A. Lebedev, O polimorfizme i otzhige stekla, *Trud. Gos. Opt. Inst.* **2**, 1 (1921) (in Russian); *Izv. Akad. Nauk SSSR, Otd. Mat. Estestv. Nauk, Ser. Fiz.* **3**, 381 (1937).
- [20] D. A. Keen and M. T. Dove, Local structures of amorphous and crystalline phases of silica, SiO<sub>2</sub>, by neutron total scattering, *J. Phys.: Condens. Matter* **11**, 9263 (1999).
- [21] M. F. Thorpe, Continuous deformations in random networks, *J. Non-Cryst. Solids* **57**, 355 (1983).
- [22] W. G. Ellenbroek, V. F. Hagh, A. Kumar, M. F. Thorpe, and M. van Hecke, Rigidity Loss in Disordered Systems: Three Scenarios, *Phys. Rev. Lett.* **114**, 135501 (2015).
- [23] L. Theran, A. Nixon, E. Ross, M. Sadjadi, B. Servatius, and M. F. Thorpe, Anchored boundary conditions for locally isostatic networks, *Phys. Rev. E* **92**, 053306 (2015).
- [24] A. Sartbaeva, S. A. Wells, A. Huerta, and M. F. Thorpe, Local structural variability and the intermediate phase window in network glasses, *Phys. Rev. B* **75**, 224204 (2007).
- [25] P. A. Madden and M. Wilson, ‘Covalent’ effects in ‘ionic’ systems, *Chem. Soc. Rev.* **25**, 339 (1996).
- [26] P. Tangney and S. Scandolo, An *ab initio* parametrized interatomic force field for silica, *J. Chem. Phys.* **117**, 8898 (2002).
- [27] A. Kumar, M. Wilson, and M. F. Thorpe, Amorphous graphene: a realization of Zachariasens glass, *J. Phys.: Condens. Matter* **24**, 485003 (2012).
- [28] J. M. Soler, E. Artacho, J. D. Gale, A. García, J. Junquera, P. Ordejón, and D. Sánchez-Portal, The siesta method for *ab initio* order-*n* materials simulation, *J. Phys.: Condens. Matter* **14**, 2745 (2002).
- [29] B. Bhattacharai and D. A. Drabold, Vibrations in amorphous silica, *J. Non-Cryst. Solids* **439**, 6 (2016).
- [30] J. A. E. Desa, A. C. Wright, J. Wong, and R. N. Sinclair, A neutron diffraction investigation of the structure of vitreous zinc chloride, *J. Non-Cryst. Solids* **51**, 57 (1982).
- [31] J. Neufeind and K.-D. Liss, Bond angle distribution in amorphous germania and silica, *Ber. Bunseng. Phys. Chem.* **100**, 1341 (1996).
- [32] C. J. Dawson, R. Sanchez-Smith, P. Rez, M. O’Keefe, and M. M. J. Treacy, *Ab initio* calculations of the energy dependence of Si–O–Si angles in silica and Ge–O–Ge angles in germania crystalline systems, *Chem. Mater.* **26**, 1523 (2014).
- [33] A. Perrakis, R. Morris, and V. S. Lamzin, Automated protein model building combined with iterative structure refinement, *Nat. Struct. Mol. Biol.* **6**, 458 (1999).
- [34] J. Towns, T. Cockerill, M. Dahan, I. Foster, K. Gaither, A. Grimshaw, V. Hazlewood, S. Lathrop, D. Lifka, G. D. Peterson *et al.*, XSEDE: accelerating scientific discovery, *Comput. Sci. Eng.* **16**, 62 (2014).